Nonlinear dynamics of a fluid-conveying curved pipe subjected to motion-limiting constraints and a harmonic excitation

Wang Lin*, Ni Qiao

Department of Mechanics, Huazhong University of Science and Technology, Wuhan 430074, People's Republic of China

Abstract

This paper investigates the dynamical behaviour of a fluid-conveying curved pipe subjected to motion-limiting constraints and a harmonic excitation. Based on a Newtonian method, the in-plane equation of motion of this curved pipe is derived. Then a set of discrete equations in spatial space obtained by the differential quadrature method (DQM) is solved numerically. Emphasis is placed on the possible dynamical behaviour of the curved pipe conveying fluid. The numerical results show that the pipe without motion-limiting constraints but with a harmonic force behaves as an ordinary linear system. If, however, the pipe is subjected to cubic motion-limiting constraints, nonlinear dynamic phenomena of the system will occur. Calculations of bifurcation diagrams, phase-plane portraits, time responses, power spectrum diagrams, and Poincaré maps of the oscillations clearly demonstrate the existence of chaotic and quasiperiodic motions. Moreover, it is shown that the route to chaos is via a sequence of period-doubling bifurcations.
© 2007 Elsevier Ltd. All rights reserved.

Keywords: Fluid-conveying curved pipe; Motion-limiting constraint; Nonlinear dynamics; Chaotic motion; DQM

1. Introduction

The vibration problem of a curved pipe conveying fluid was investigated to a great extent in the past decades. Work on this topic originated in the early 1960s. The pioneering works on the stability of curved pipes conveying fluid were confined to the linear aspects of this fluid–structure interaction system. Afterwards, attention was focused on formulating the linear equations of motion of curved pipes. Chen (1972a, b, 1973) has studied the governing equations of uniformly curved pipes, both for the in-plane and out-of-plane vibrations, and it was found that the curved pipe might be subject to divergent or flutter instabilities. Misra et al. (1988a, b) modelled a curved pipe conveying fluid with complex shape by the finite element method, taking into account the steady-state combined tension–pressure forces, neglected by Chen. Dupuis and Rousselet (1985) utilized a transfer matrix method to investigate the dynamics of curved pipes. Subsequently, Aithal and Gipson (1990) studied a semicircular pipe conveying fluid by an analytical method. Recently, Ni and Huang (2000) used the differential quadrature method (DQM) to calculate the critical fluid velocity of a curved pipe with a linear spring support.

On the other hand, the literature on nonlinear vibrations of fluid-conveying curved pipes is limited. Perhaps the earliest study on the nonlinear problem of a curved pipe was by Ko and Bert (1984). Subsequently, Ko and Bert (1986) considered

---

*Corresponding author. Fax: +86 27 87543238.
E-mail address: wanglinfliping@sohu.com (W. Lin).

the first-order nonlinear interaction between the pipe structure and the flowing fluid and obtained the governing equations for the in-plane vibrations of a circular-arc pipe containing flowing fluid. In a notable work, Dupuis and Rousselet (1992) derived the nonlinear differential equation of motion for a fluid-conveying pipe by making use of the Newtonian method. However, from a literature survey, it is found that the work dealing with the chaotic motions of curved pipes conveying fluid is quite limited. The bifurcations and chaotic regime in curved pipes have not been revealed yet.

The main aim of the present study is to explore the dynamics of a curved pipe conveying fluid. First, the derivation of the equation of motion is carried out for a fluid-conveying curved pipe with motion-limiting constraints. This equation of motion is obtained by means of the Newtonian force–moment balance method and a comparison with existing derivations is made. Second, the DQM is utilized to discretize the pipe model, in which the harmonic excitation is considered. This numerical method has been used to analyse the linear stability of curved pipe conveying fluid (Ni and Huang, 2000). It is very convenient to deal with the equation of motion and the corresponding boundary conditions of the curved pipe by the DQM. Third, the linear responses and nonlinear behaviour, corresponding to the linear and nonlinear systems under consideration, are investigated by changing several key parameters. Numerical results are presented to show some interesting and unexpected dynamical behaviour, which will be described in the following sections.

2. Formulation of the equation of motion

A semicircular fluid-conveying curved pipe of constant centre-line radius R to a fixed geometric centre of curvature at point O, as shown in Fig. 1, is considered. The pipe subjected to motion-limiting constraints at θ_c is forced by a harmonic excitation in the radial direction at the free end of the pipe. The analytical model consists of a curved pipe having a mass per unit length m_p, effective flexural rigidity EI, internal perimeter S, and internal cross-sectional area A. For simplicity, the fluid is taken to be incompressible and in laminar flow with a mass per unit length m_f, and constant velocity V. The fluid pressure is denoted by p.

This analysis is carried out for the in-plane vibrational motion of such a fluid–structure system. We denote the radial deflection and tangential displacement of the curved pipe as u and w, respectively. According to Timoshenko and Gere (1961), for one element of the curved pipe, the radius of curvature after deformation can be given by the following relationship:

$$\frac{1}{R'} = \frac{1}{R}\left(1 + \frac{u}{R} + \frac{1}{R}\frac{\partial^2 u}{\partial \theta^2}\right). \tag{1}$$

The relation between the radial deflection and the tangential displacement can be obtained by the condition of inextensibility (Love, 1927):

$$u = \frac{\partial w}{\partial \theta}. \tag{2}$$

Let F, T, and M denote the internal shear force, normal force, and bending moment, respectively. The differential equations for rotational motion and for translational motions in radial and tangential directions of the element are:

$$\frac{\partial M}{\partial \theta} + RF = 0, \tag{3}$$

$$\frac{\partial F}{\partial \theta} + T - RQ - fR = m_p R \frac{\partial^2 u}{\partial t^2}, \tag{4}$$
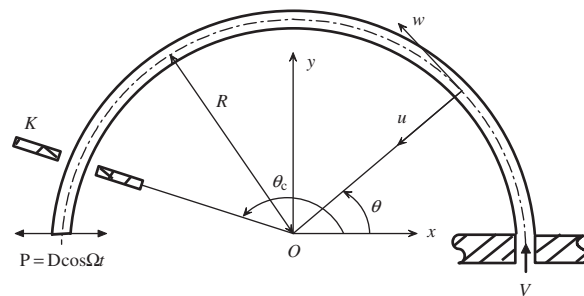

Fig. 1. Schematic of the dynamical system.

$$\frac{\partial T}{\partial \theta} + RSq - F = m_p R \frac{\partial^2 w}{\partial t^2}, \tag{5}$$

in which q is the shear stress on the internal surface of the pipe, Q the transverse force per unit length between pipe wall and fluid, and f represents the effect of motion-limiting constraints which can be written as the restraining force:

$$f = Ku^3 \delta(\theta - \theta_c), \tag{6}$$

where K is the stiffness of the cubic spring, and δ the Dirac delta function.

Similarly, consider the fluid element (see Fig. 2). The accelerations of a fluid particle in the tangential and radial directions are, respectively,

$$\frac{\partial^2 w}{\partial t^2} - \frac{V^2}{R^2}\left(\frac{\partial^2 w}{\partial \theta^2} + w\right) \quad \text{and} \quad \frac{V^2}{R}\left(1 + \frac{u}{R}\right) + \left(\frac{\partial}{\partial t} + \frac{V}{R}\frac{\partial}{\partial \theta}\right)^2 u + \frac{2V}{R}\frac{\partial w}{\partial t}.$$

Hence, in terms of the force balances in the radial and tangential directions, one obtains:

$$Q - \frac{PA}{R'} = \frac{m_f V^2}{R}\left(1 + \frac{u}{R}\right) + m_f\left(\frac{\partial^2 u}{\partial t^2} + \frac{2V}{R}\frac{\partial^2 u}{\partial t \partial \theta} + \frac{2V}{R}\frac{\partial w}{\partial t} + \frac{V^2}{R^2}\frac{\partial^2 u}{\partial \theta^2}\right), \tag{7}$$

$$A\frac{\partial p}{\partial \theta} + RSq = -m_f R\left[\frac{\partial^2 w}{\partial t^2} - \frac{V^2}{R^2}\left(\frac{\partial^2 w}{\partial \theta^2} + w\right)\right]. \tag{8}$$

In converting these force and moment equations to displacement equations, the relation of moment and deflection is introduced as follows:

$$M = \frac{EI}{R^2}\left\{\left(\frac{\partial^2 u}{\partial \theta^2} + \frac{\partial w}{\partial \theta}\right)\Big/\left[1 - \frac{u}{R}\right]\right\}. \tag{9}$$
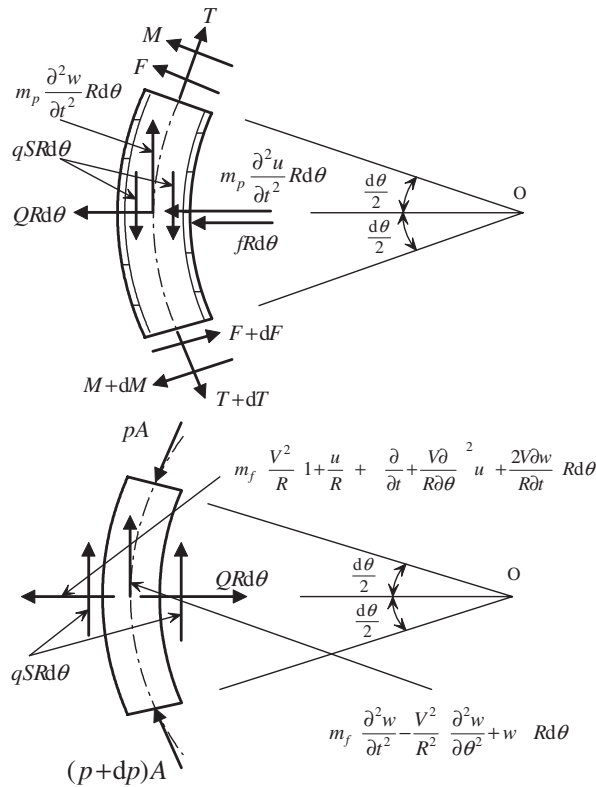

Fig. 2. Forces and moments acting on elements of the pipe and the fluid.

If the initial radius of curvature of the pipe is relatively large compared to the displacements, the ratio between displacement and the initial radius of curvature of the pipe becomes a higher-order term and can reasonably be neglected as suggested by Timoshenko and Gere (1961). Thus, Eq. (9) can be approximated by the following expression:

$$M = \frac{EI}{R^2}\left(\frac{\partial^2 u}{\partial \theta^2} + \frac{\partial w}{\partial \theta}\right). \tag{10}$$

By utilizing Eqs. (1), (2), (6), and (10), Eqs. (3)–(5), (7), and (8) can be reduced to a single sixth-order partial differential equation for w. The equation is:

$$\begin{aligned}
&\frac{\partial^6 w}{\partial \theta^6} + \left(2 + \frac{AR^2 p}{EI} + \frac{m_f R^2 V^2}{EI}\right)\frac{\partial^4 w}{\partial \theta^4} + \left(1 + \frac{AR^2 p}{EI} + \frac{2m_f R^2 V^2}{EI}\right)\frac{\partial^2 w}{\partial \theta^2} + \frac{m_f R^2 V^2}{EI} w \\
&+ \frac{2m_f R^3 V}{EI}\frac{\partial^4 w}{\partial t \partial \theta^3} + \frac{2m_f R^3 V}{EI}\frac{\partial^2 w}{\partial t \partial \theta} + \frac{(m_f + m_p)R^4}{EI}\frac{\partial^4 w}{\partial t^2 \partial \theta^2} - \frac{(m_f + m_p)R^4}{EI}\frac{\partial^2 w}{\partial t^2} \\
&+ \frac{3R^4}{EI}\left[K\left(\frac{\partial w}{\partial \theta}\right)^2\frac{\partial^2 w}{\partial \theta^2}\right]\delta(\theta - \theta_c) + \frac{R^4}{EI}\left[K\left(\frac{\partial w}{\partial \theta}\right)^3\right]\frac{\partial \delta(\theta - \theta_c)}{\partial \theta} = 0.
\end{aligned} \tag{11}$$

Compared with the linear equation of motion derived by Chen (1972b), the only nonlinearity in the above equation is associated with the nonlinear constraints. Hence, Eq. (11) should be valid only provided that the pipe motions are not too large. Another aspect is that this equation does not take into account the effect of steady-state axial tension and pressure that may cause a steady-state deformation of the curved pipe. Since the boundary conditions considered in this study are clamped-free conditions, the steady-state axial tension–pressure force has a less pronounced effect on a clamped-free curved pipe (Misra et al., 1988a). Therefore, the use of Eq. (11) can reasonably capture the main characteristics of the cantilever system. One can also consult the book by Païdoussis (1998), which contains extensive discussion of various issues related to the modelling of fluid-conveying curved pipes.

By setting the fluid pressure equal to zero, upon introducing the dimensionless parameters, Eq. (11) reduces to

$$\begin{aligned}
&\frac{1}{\pi^6}\frac{\partial^6 \xi}{\partial \zeta^6} + (2 + v^2)\frac{1}{\pi^4}\frac{\partial^4 \xi}{\partial \zeta^4} + (1 + 2v^2)\frac{1}{\pi^2}\frac{\partial^2 \xi}{\partial \zeta^2} + v^2 \xi + 2\beta^{1/2}v\frac{1}{\pi^3}\frac{\partial^4 \xi}{\partial \tau \partial \zeta^3} + 2\beta^{1/2}v\frac{1}{\pi}\frac{\partial^2 \xi}{\partial \tau \partial \zeta} \\
&+ \frac{1}{\pi^2}\frac{\partial^4 \xi}{\partial \tau^2 \partial \zeta^2} - \frac{\partial^2 \xi}{\partial \tau^2} + 3\left[k\frac{\partial^2 \xi}{\partial \zeta^2}\left(\frac{\partial \xi}{\partial \zeta}\right)^2\right]\delta(\zeta - \zeta_c) + \left[k\left(\frac{\partial \xi}{\partial \zeta}\right)^3\right]\frac{\partial \delta(\zeta - \zeta_c)}{\partial \zeta} = 0,
\end{aligned} \tag{12}$$

in which the dimensionless parameters are defined as

$$\begin{aligned}
&\xi = w/R, \quad \eta = u/R, \quad \zeta = \theta/\pi, \quad \beta = m_f/(m_f + m_p), \quad v = (m_f/EI)^{1/2}RV, \\
&\tau = \left[EI/(m_f + m_p)\right]^{1/2}t\big/R^2, \quad k = K\big(R^6/EI\pi^5\big), \quad \zeta_c = \theta_c/\pi.
\end{aligned} \tag{13}$$

The governing equation, Eq. (12), is a nonlinear differential equation and its solution is associated with the boundary conditions of the pipe system. Let $\tilde{\psi}, \tilde{N}, \tilde{M},$ and $\tilde{Q}$ be the angle of rotation, axial force, bending moment and transverse shear force, respectively. For this pipe model, the boundary conditions to be satisfied are as follows:

At the fixed end ($\theta = 0$):

$$u = w = 0, \quad \tilde{\psi} = \frac{\partial u}{R\partial \theta} = 0. \tag{14}$$

At the free end ($\theta = \pi$):

$$\tilde{M} = \frac{EI}{R^2}\left(\frac{\partial^3 w}{\partial \theta^3} + \frac{\partial w}{\partial \theta}\right) = 0, \quad \tilde{Q} = \frac{EI}{R^3}\left(\frac{\partial^4 w}{\partial \theta^4} + \frac{\partial^2 w}{\partial \theta^2}\right) = D\cos(\Omega t), \tag{15,16}$$

$$\begin{aligned}
\tilde{N}_\pi &= \frac{EI}{R^4}\left(\frac{\partial^5 w}{\partial \theta^5} + 2\frac{\partial^3 w}{\partial \theta^3} + \frac{\partial w}{\partial \theta}\right) + \frac{m_f V^2}{R^2}\left(\frac{\partial^3 w}{\partial \theta^3} + \frac{\partial w}{\partial \theta}\right) + \frac{2m_f V}{R}\frac{\partial^3 w}{\partial \theta^2 \partial t} \\
&+ \frac{m_f V}{R}\frac{\partial w}{\partial t} + (m_f + m_p)\frac{\partial^3 w}{\partial \theta \partial t^2} + \frac{m_f V}{R}\left(\frac{\partial w}{\partial t} + V\right) = 0.
\end{aligned} \tag{17}$$

Note that the term on the right-hand side of Eq. (16), $D\cos(\Omega t)$, denotes the harmonic excitation at the free-end of the pipe. Thus, the boundary conditions can be rewritten as the dimensionless form:

$$\xi(0,\tau) = \eta(0,\tau) = \frac{\partial \eta(0,\tau)}{\partial \zeta} = 0, \tag{18}$$

$$\frac{1}{\pi^3}\frac{\partial^3 \xi(1,\tau)}{\partial \zeta^3} + \frac{1}{\pi}\frac{\partial \xi(1,\tau)}{\partial \zeta} = 0, \tag{19}$$

$$\frac{1}{\pi^4}\frac{\partial^4 \xi(1,\tau)}{\partial \zeta^4} + \frac{1}{\pi^2}\frac{\partial \xi^2(1,\tau)}{\partial \zeta^2} = d\,\cos(\omega\tau), \tag{20}$$

$$\frac{1}{\pi^5}\frac{\partial^5 \xi(1,\tau)}{\partial \zeta^5} + \frac{1}{\pi^3}\frac{\partial \xi^3(1,\tau)}{\partial \zeta^3} + 2\beta^{1/2}v\frac{1}{\pi^2}\frac{\partial \xi^3(1,\tau)}{\partial \tau \partial \zeta^2} + 2\beta^{1/2}v\frac{\partial \xi(1,\tau)}{\partial \tau} + \frac{1}{\pi}\frac{\partial \xi^3(1,\tau)}{\partial \tau^2 \partial \zeta} + v^2 = 0, \tag{21}$$

where $d = DR^3/EI$, $\omega = [(m_f + m_p)/EI]^{1/2}R^2\Omega$.

3. Discretization of the fluid-conveying curved pipe

In this section, the DQM is introduced to discretize the equation of motion of the curved pipe. The differential quadrature technique approximates the partial derivative of a function with respect to a space variable at a given discrete point as a weighted linear sum of the function values at all discrete points in the domain of that variable. This is in contrast to the finite difference method in which a solution value at a point is a function of values at adjacent points only. Even if the finite difference method is of high enough order to cover all points on the grid, a fundamental difference remains in that the method of differential quadrature is a polynomial fitting, while the higher-order finite difference method is a Taylor series expansion. Mathematically, the application of the DQM to a partial differential equation can be expressed as follows:

$$L_k\{f(x)\}_i = \sum_{j=1}^{N} A_{ij}^{(k)}f(x_j), \tag{22}$$

where L denotes a differential operator, k is the kth order of derivative, x_j $(j = 1, 2, \ldots, N)$ are the discrete points considered in the domain, $f(x_j)$ are the function values at these points, $A_{ij}^{(k)}$ are the weighting coefficients attached to these function values, and N denotes the number of discrete points in the domain. Note that the weighting coefficients have been given by Bert and Malik (1996).

For the curved pipe, the discrete points are in the domain of ζ. By using the following method to discretize $\zeta(0 \leqslant \zeta \leqslant 1)$, one obtains the unequally spaced sampling points with three adjacent Δ-points ($\Delta = 10^{-6} \sim 10^{-3}$) at the two boundary ends, namely

$$\zeta_1 = 0, \quad \zeta_2 = \Delta, \quad \zeta_3 = 2\Delta, \quad \zeta_{N-2} = 1 - 2\Delta, \quad \zeta_{N-1} = 1 - \Delta, \quad \zeta_N = 1,$$

$$\zeta_i = \frac{1}{2}\left[1 - \cos\left(\frac{i-3}{N-4}\pi\right)\right], \quad (i = 4, 5, \ldots, N-3). \tag{23}$$

For simplicity, the motion-limiting constraints are applied at the point where $c = N-3$. Applying the DQM to Eq. (12) yields:

$$\sum_{j=1}^{N}\left[\frac{1}{\pi^6}A_{ij}^{(6)} + \frac{1}{\pi^4}(2+v^2)A_{ij}^{(4)} + \frac{1}{\pi^2}(1+2v^2)A_{ij}^{(2)}\right]\xi_j + v^2\xi_i + 2\beta^{1/2}v\sum_{j=1}^{N}\left(\frac{1}{\pi^3}A_{ij}^{(3)} + \frac{1}{\pi}A_{ij}^{(1)}\right)\dot{\xi}_j + \sum_{j=1}^{N}\frac{1}{\pi^2}A_{ij}^{(2)}\ddot{\xi}_j - \ddot{\xi}_i$$

$$+ 3k\left(\sum_{j=1}^{N}A_{cj}^{(1)}\xi_j\right)^2\left(\sum_{j=1}^{N}A_{cj}^{(2)}\xi_j\right) + kA_{cc}^{(1)}\left(\sum_{j=1}^{N}A_{cj}^{(1)}\xi_j\right)^2\left(\sum_{j=1}^{N}A_{cj}^{(1)}\xi_j\right) = 0, \quad (i = 4, 5, \ldots, N-3). \tag{24}$$

The boundary conditions of the pipe, given by Eqs. (18)–(21), can be expressed in the differential quadratue form as follows:

$$\xi_1 = 0, \quad \sum_{j=1}^{N}A_{2j}^{(1)}\xi_j = 0, \quad \sum_{j=1}^{N}A_{3j}^{(2)}\xi_j = 0, \tag{25}$$

$$\sum_{j=1}^{N} \frac{1}{\pi^3} A_{(N-2)j}^{(3)} \xi_j + \sum_{j=1}^{N} \frac{1}{\pi} A_{(N-2)j}^{(1)} \xi_j = 0, \qquad (26)$$

$$\sum_{j=1}^{N} \frac{1}{\pi^4} A_{(N-1)j}^{(4)} \xi_j + \sum_{j=1}^{N} \frac{1}{\pi^2} A_{(N-1)j}^{(2)} \xi_j = d \cos(\omega\tau), \qquad (27)$$

$$\sum_{j=1}^{N} \frac{1}{\pi^5} A_{Nj}^{(5)} \xi_j + \sum_{j=1}^{N} \frac{1}{\pi^3} A_{Nj}^{(3)} \xi_j + 2\beta^{1/2} v \sum_{j=1}^{N} \frac{1}{\pi^2} A_{Nj}^{(2)} \dot{\xi}_j + \dot{\xi}_N + \sum_{j=1}^{N} \frac{1}{\pi} A_{Nj}^{(1)} \ddot{\xi}_j + v^2 = 0. \qquad (28)$$

Hence, by rearranging Eqs. (24)–(28), an assembled form of the dynamic motion equation is given as follows:

$$[M]\{\ddot{\xi}\} + [G]\{\dot{\xi}\} + [K]\{\xi\} = \{Q\}, \qquad (29)$$

in which $\{\xi\}$, $\{\dot{\xi}\}$, and $\{\ddot{\xi}\}$ are the structural displacement, velocity, and acceleration vectors, respectively; $[M]$, $[G]$, $[K]$, and $[Q]$ denote the structural mass matrix, damping matrix, stiffness matrix and forcing vector, respectively. The matrix elements of $[G]$ and $[K]$ are functions of the dimensionless fluid speed v and mass ratio β. Moreover, $[K]$ can be written as

$$[K] = [K_l] + [K_{nl}], \qquad (30)$$

where $[K_l]$ and $[K_{nl}]$ are the linear and nonlinear terms of $[K]$, respectively. Obviously, all the elements of $[M]$, $[G]$, $[K]$, and $[Q]$ can be obtained directly from Eqs. (24)–(28). Eq. (29) is the nonlinear dynamic equation of motion for the curved pipe conveying fluid. By solving this equation one can determine the dynamical behaviour of the curved pipe under certain conditions.

As mentioned in the foregoing, the tangential displacement and the radial displacement of the curved pipe are interrelated. If the time response of the tangential displacement is determined by solving Eq. (29), the radial displacement can be obtained by the following relationship:

$$\eta_i = \sum_{k=1}^{N} A_{ik}^{(1)} \xi_k, \quad (i = 1, 2, \ldots, N). \qquad (31)$$

4. Numerical results

In this section, it is of interest to investigate, in detail, what behaviour may occur when several parameter values are varied. For this purpose, the Newmark method and Newton–Raphson iterative technique were used to develop the procedure for such a fluid–structure interaction system governed by Eq. (29).

In what follows, results will be presented for two cases. The first case is the investigation of the linear system with no motion-limiting constraints ($k = 0$). It should be noted that, when the curved pipe with no motion-limiting constraint loses stability, the fluid velocity would be sufficiently high and the tip displacement of the vibrating pipe becomes large. Eq. (12) could not, exactly, describe the vibrations of the pipe system with large displacement, since the geometric nonlinearity of the pipe is not considered. Calculations of critical fluid velocities and analysis of linear parametric instability have less practical significance, as Eq. (12) cannot represent the true situation for instability of the pipe. In the present paper, the linear analysis is limited to the curved pipe conveying fluid with low velocity. Thus, the parametric instabilities will not be considered in the linear analysis. In fact, to study the parametric instability of curved pipe with no motion-limiting constraints, pipe models with geometric nonlinearities should be developed.

The second case is to explore the nonlinear dynamics of the constrained pipe, both without and with a harmonic excitation.

4.1. Linear analysis

To check the numerical scheme, the linear system will be investigated first. We take the value of $k = 0$; thus, the equation of motion is kept linear. If the forcing function (harmonic excitation) is absent, Eq. (12) can be reduced to that obtained by Chen (1972a). It should be pointed out that, for a cantilevered curved pipe, Chen (1972a) had obtained the static deflections of the curved pipe. These static deflections were shown to be related to the fluid velocity. If the fluid velocity was increased gradually, the static deflections became larger. Therefore, when the fluid velocity was sufficiently high, the cantilever system was predicted to be subject to flutter with large displacement. In this study, only small displacement will be considered, both for the linear and nonlinear systems.
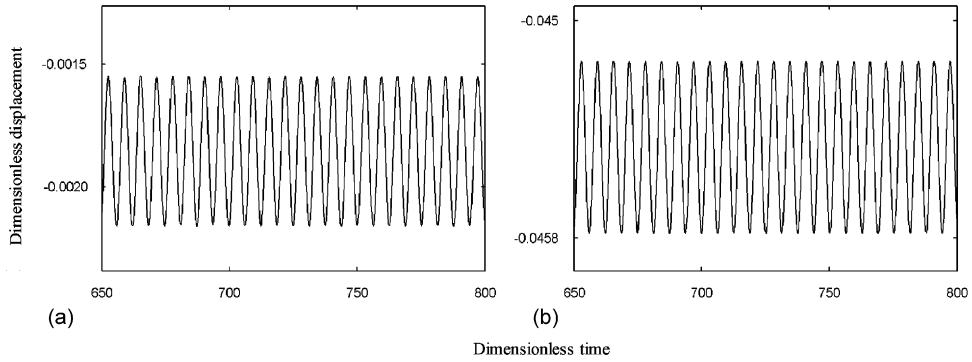
Fig. 3. Time responses for the tip displacement of the linear system defined by $d = 0.005$, $\omega = 1$. (a) $v = 0.02$; (b) $v = 0.1$.
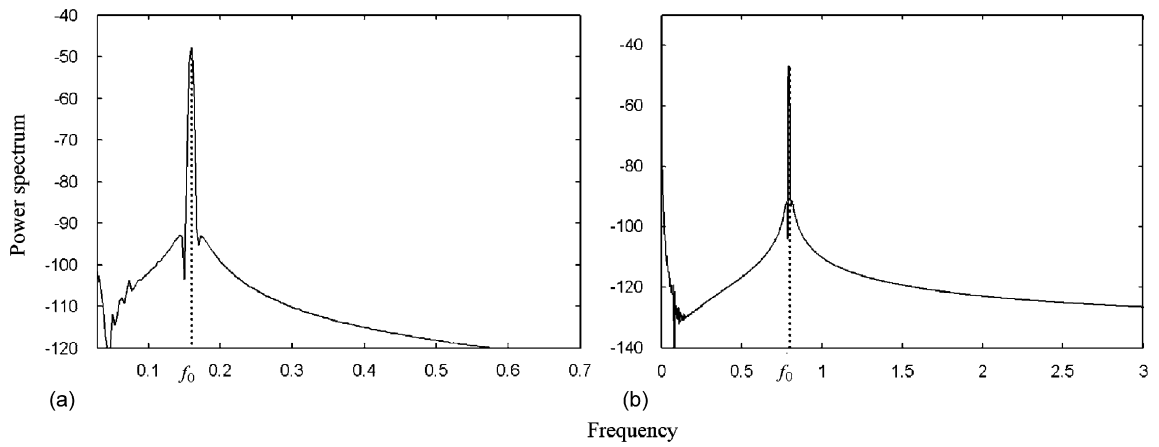

Fig. 4. Power spectrrums for the tip displacement of the linear system defined by $d = 0.005$, $v = 0.1$. (a) $\omega = 1$; (b) $\omega = 5$.
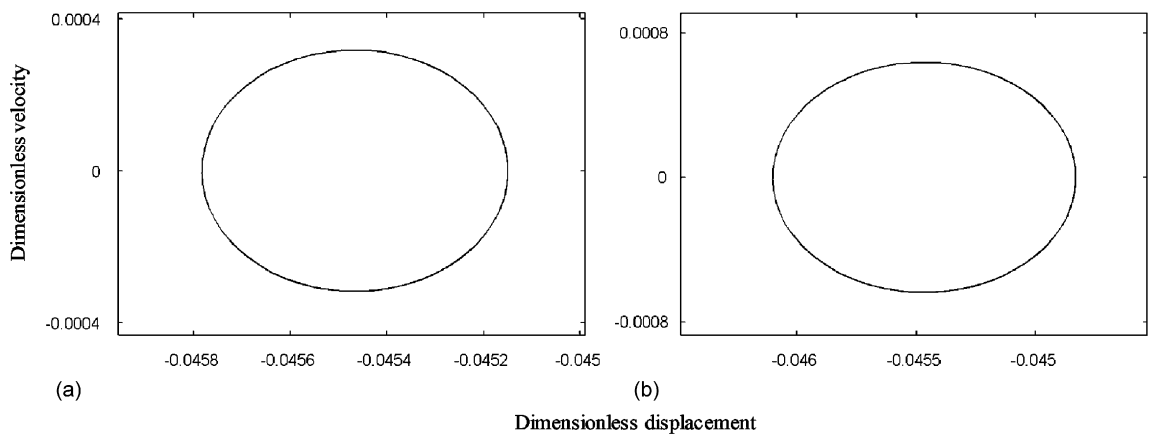

Fig. 5. Phase-plane portraits for the tip displacement of the linear system defined by $\omega = 1$, $v = 0.1$. (a) $d = 0.005$; (b) $d = 0.01$.

In the linear analysis, one important aspect is to explore the effect of forcing function on the dynamics of the linear system. For this purpose, we choose $\beta = 0.5$ and $N = 12$ for the calculations. Firstly, for $d = 0.005$, $\omega = 1$, and $v = 0.02$, the curved pipe will undergo a limit cycle motion. The centre of the limit cycle is not at the origin of the phase

plane, as can be seen in Fig. 3(a). However, there exists a distance between these two points (the centre of the limit cycle and the origin of the phase plane). If the fluid speed becomes slightly higher (e.g., $v = 0.1$), the distance becomes larger; but the radius of the limit cycle still remains constant (see Fig. 3(b)). Then the time response of the vibrations can be obtained with fixed values of v and d. Sample results are shown in Figs. 4(a) and (b), corresponding to two different values of ω. In Figs. 4(a) and (b), it is observed that the vibrating frequency of the system and the forcing frequency is related by $f_0 = \omega/2\pi$. Moreover, for the case $\omega = 1$, the vibrating frequency equals $\frac{1}{5}$ of that for the case $\omega = 5$. This means that the vibrating frequency of the system is dominated by the forcing function. As expected, it is also observed that the radius of the limit cycle is associated with the forcing amplitude d, i.e., the radius increases with increasing forcing amplitude. Typical results are presented in Figs. 5(a) and (b).

4.2. Nonlinear dynamics

4.2.1. Without forcing function

In the nonlinear analysis, the dynamics of the curved pipe system with no forcing function will be examined first. For this purpose, the bifurcation diagram is constructed via numerical calculations. Construction of a bifurcation diagram is a standard approach used to analyse various nonlinear systems. In a bifurcation diagram, the dynamical behaviour may be viewed globally over a range of parameter values and allows us to compare simultaneously different types of motion. Thus, the bifurcation diagram provides a summary of essential dynamics and is therefore a useful tool for acquiring an overview.

Calculations have produced the bifurcation diagram of Fig. 6 for a set of system parameters defined as follows:

$$\beta = 0.5, \quad k = 1000, \quad \zeta_c = 0.854, \quad N = 12, \quad d = 0.0, \quad \omega = 0. \tag{32}$$

In the bifurcation diagram, in the ordinate is the amplitude of the free-end displacement of the pipe. In the calculations, for clarity, the transient solutions were discarded. Then, whenever the free-end velocity, $\dot{\xi}(1,\tau)$, was zero, the displacement at the free end was recorded—thus, producing both positive and negative values, as shown in Fig. 6. In this figure, the varied parameter is the dimensionless fluid speed v, and all the other parameters are defined by Eq. (32). From the bifurcation diagram, one can clearly see that the pipe holds still when the fluid speed is low (i.e., $v < 0.2383$). It should be mentioned that, for low fluid speeds, perhaps the system settles down onto the constraints with a negative static deflection (see Fig. 6). However, when the fluid speed increases to $v = 0.2383$, a limit cycle motion can be detected. Furthermore, the amplitude of the limit cycle increases with increasing fluid speed. For a higher v, a sequence of period-doubling bifurcations is visible in Fig. 6, leading to chaotic motions. Several typical phase-plane portraits of these interesting motions are shown in Fig. 7.

4.2.2. With forcing function

4.2.2.1. Bifurcation diagram.
In the foregoing, the nonlinear pipe system with no forcing function has been investigated, and the bifurcations and several motions were discussed. However, if the nonlinear system is subject to a
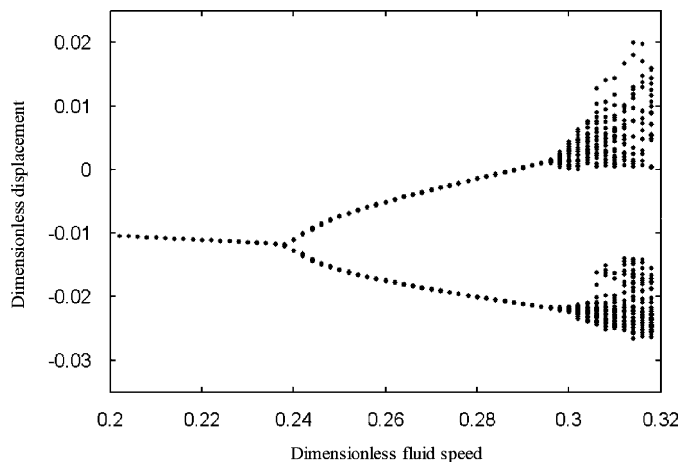

Fig. 6. Bifurcation diagram for the tip displacement of the nonlinear system defined by Eq. (32), as fluid speed is varied.

harmonic excitation at the tip, the modified system may display much richer dynamics, as described in the following.
A bifurcation diagram may be constructed for another set of system parameters defined as follows (Fig. 8):

$$\beta = 0.5, \quad k = 1000, \quad \zeta_c = 0.854, \quad N = 12, \quad d = 0.005, \quad \omega = 1. \tag{33}$$

Obviously, in the results presented in Fig. 8, the harmonic excitation is nonzero. Except for the forcing amplitude and forcing frequency, all the other parameters utilized are chosen to be the same as those defined by Eq. (32). For a small value of v (e.g., $v = 0.0001$), the pipe undergoes a symmetric limit cycle motion. However, the limit cycle motion becomes asymmetric when the fluid speed is increased. For $v > 0.0674$, short chaotic bursts occur, with several regions of
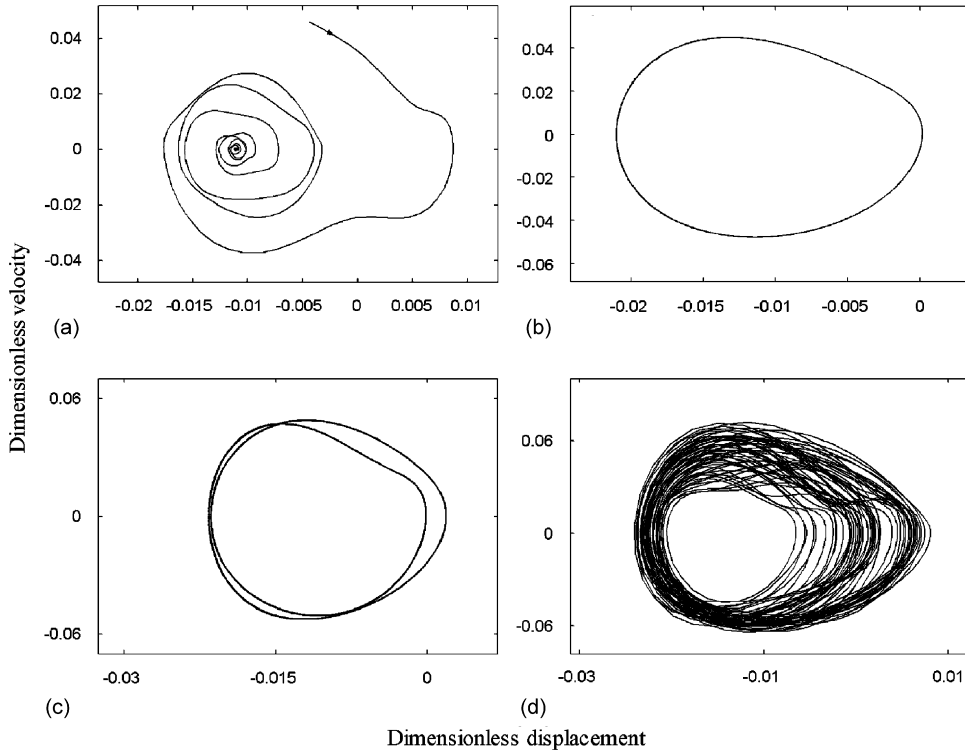

Fig. 7. Phase-plane plots of the free-end deflection of the pipe, for the system of Fig. 6, and various values of v: (a) $v = 0.22$; (b) $v = 0.29$; (c) $v = 0.295$; (d) $v = 0.304$.
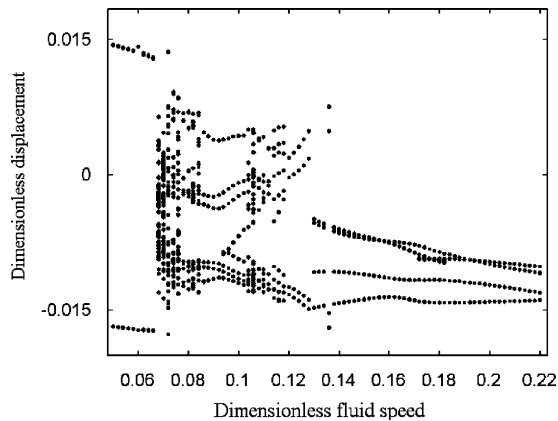

Fig. 8. Bifurcation diagram for the tip displacement of the nonlinear system defined by Eq. (33), as v is varied.
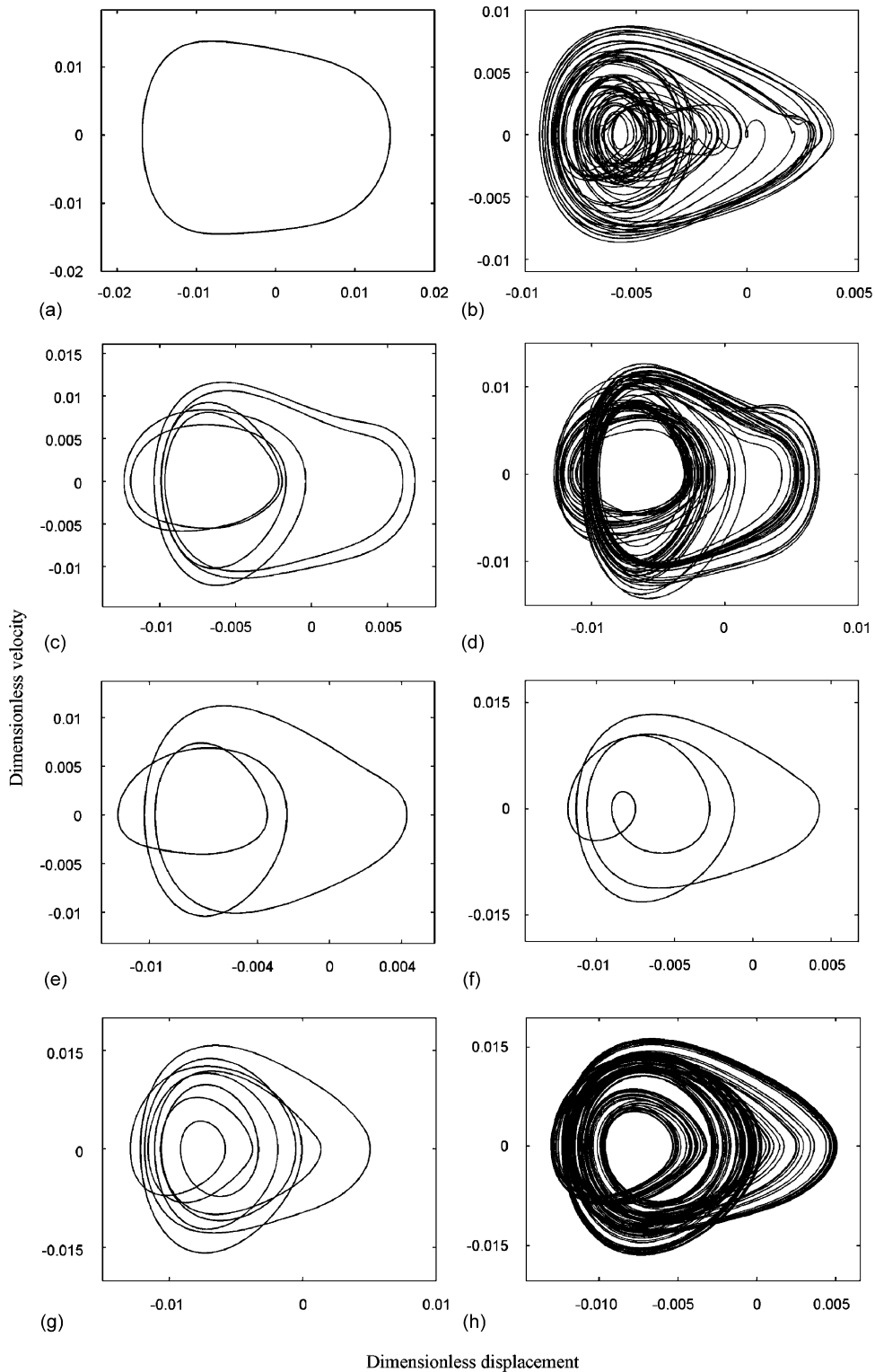
Fig. 9. Phase-plane plots of the free-end deflection of the pipe, for the system of Fig. 8, and various values of v: (a) $v = 0.05$, (b) $v = 0.068$, (c) $v = 0.078$, (d) $v = 0.082$, (e) $v = 0.088$, (f) $v = 0.098$, (g) $v = 0.104$, (h) $v = 0.106$, (i) $v = 0.130$, (j) $v = 0.220$, (k) $v = 0.240$, (l) $v = 0.260$, (m) $v = 0.270$, (n) $v = 0.290$.
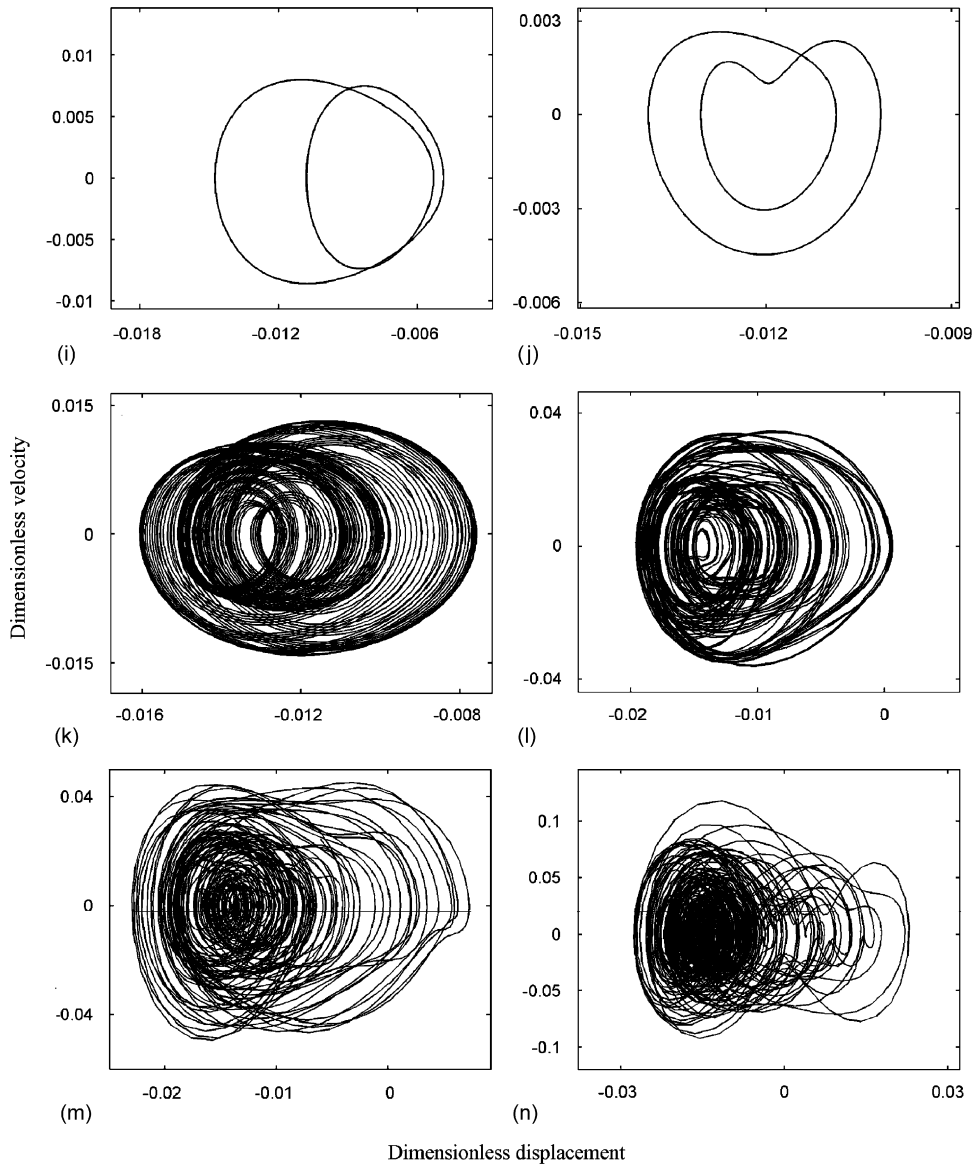
Fig. 9. (*Continued*)

periodic motions embedded within the chaotic region. In the range $0.19 < v < 0.22$, the pipe undergoes a period-2 motion, which can be clearly seen in the bifurcation diagram. When v is increased further, the period-2 motion is interrupted by a short quasiperiodic burst. This quasiperiodic motion finally evolves to a chaotic motion (the quasiperiodic and subsequent chaotic motions are not plotted in the bifurcation diagram, but can be seen in Fig. 9). For the bifurcation diagram, it should be pointed out that many discontinuities (jumps) arise in the region of v, the nature of which is not understood yet and needs further investigation.

4.2.2.2. Several interesting dynamic motions. As mentioned in the foregoing, the curved pipe may undergo various motions as the parameter v is varied. In the following, it is instructive to look at several typical motions of the pipe system. For this purpose, the phase-plane portraits were constructed, corresponding to different dynamical motions as discussed in the foregoing. The results of phase-plane portraits are shown in Fig. 9. It is seen in Fig. 9(a) that the trajectory is a stable limit cycle, which is asymmetric. The remaining parts of Fig. 9, show the following: (b), (d), (h),

and (l)–(n) show chaotic motions with various values of v; (c), (e), (f), (g), (i), and (j) show, respectively, period-6, -3, -4, -8, -2, and -2 motions; (k) shows a quasiperiodic motion. The Poincaré map and power spectrum diagram of the quasiperiodic motion will be given later.

More extensive calculations have produced the time responses, power spectrum diagrams and Poincaré maps for several typical motions. Sample results are shown in Figs. 10–12. Note that the periodic or quasiperiodic motion results in a power spectrum function that has limited frequency bandwidth. For the chaotic motion, however, the power spectrum function has a broad frequency bandwidth, which can be seen in Fig. 11. Moreover, from Fig. 12, one can see that the Poincaré map of the quasiperiodic motion is a closed curve; however, the Poincaré map of the chaotic motion has spread out and contains an infinite number of points.
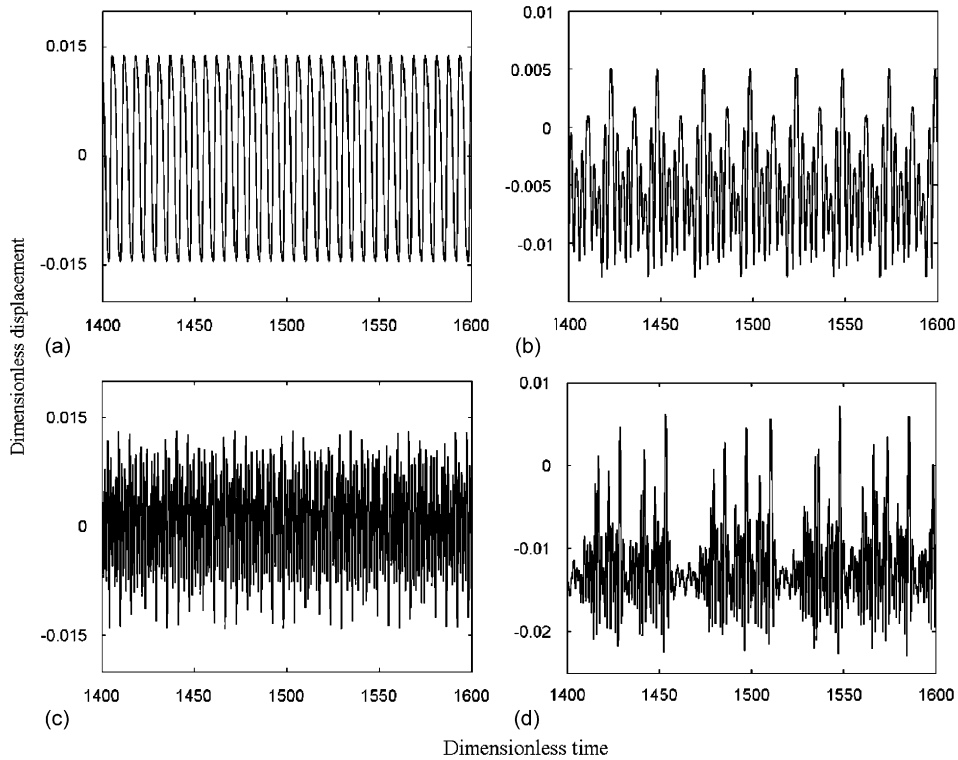

Fig. 10. Time responses for the free-end displacement of the pipe, for the system of Fig. 8. (a) $v = 0.05$, period-1 motion; (b) $v = 0.1046$, period-16 motion; (c) $v = 0.240$, quasi-periodic motion; (d) $v = 0.270$, chaotic motion.
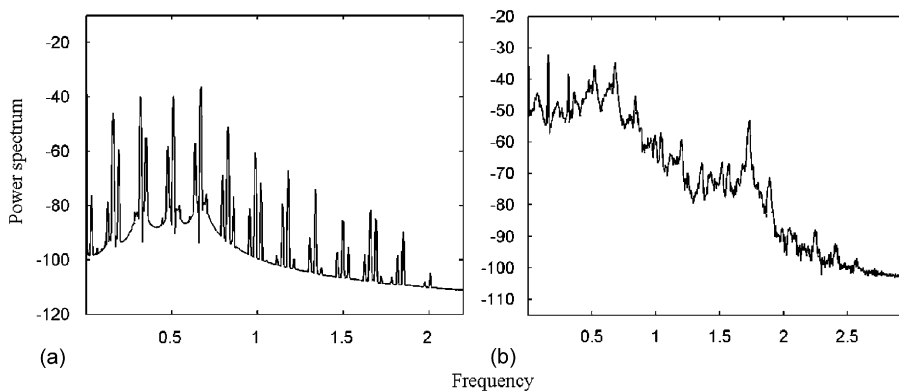

Fig. 11. . Power spectrums of the vibration, for the system of Fig. 8. (a) $v = 0.240$, (b) $v = 0.270$.
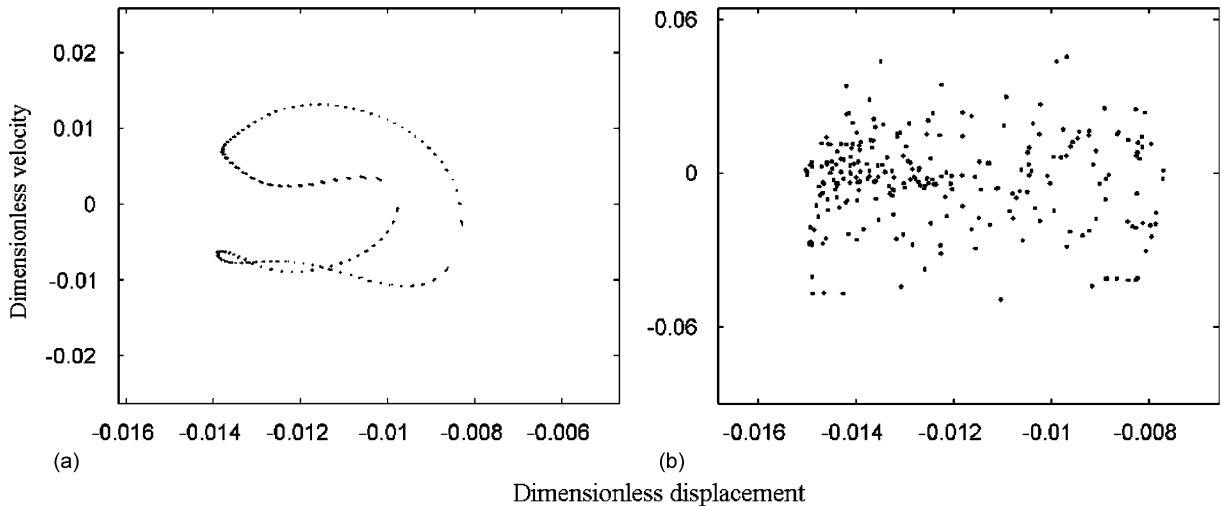
Fig. 12. . Poincare maps for the free-end displacement and velocity, for the system of Fig. 8. (a) $v = 0.240$, (b) $v = 0.270$.

4.2.2.3. The route to chaos.   In the numerical calculations, it is found that, as the parameter v varies from a very small value to a reasonably large one, chaotic motions occur following a particular route. When the value of v varies in the range $0.09 < v < 0.1062$, a sequence of period-doubling bifurcations can be detected, leading to a chaotic regime finally.

For $v = 0.270$, if the only parameter varied is chosen to be the forcing frequency and the other parameters are fixed as defined in Eq. (33), quasiperiodic motion can also be found in the parameter space of ω. Moreover, the quasiperiodic and chaotic motions have been detected to occur alternately as ω is varied continuously. Sample results are shown in Fig. 13. However, how the chaotic responses are created by following the quasiperiodic motions as ω is varied is still not understood, and it needs our further investigation.

4.2.2.4. Summary.   From the numerical results represented previously, two variants of the basic system (linear system) were considered. One is a curved pipe system with motion-limiting constraints and a harmonic excitation, and another is a curved pipe system with motion-limiting constraints but without harmonic excitation. There exist strong contrasts between these two variants of the pipe system. As can be seen from the bifurcation diagrams, for the constrained pipe with a harmonic excitation, there exist many discontinuities as opposed to no discontinuities for the constrained pipe without harmonic excitation. The global and detailed dynamics of these two variants are also different from each other.

5. Discussion and conclusions

In this paper, the dynamical behaviour of a fluid-conveying curved pipe subjected to motion-limiting constraints and a harmonic excitation has been investigated. Particular attention is concentrated on the possible existence of chaotic oscillations and several other interesting motions.

The equation of motion derived by the Newtonian method is discretized by the DQM and then the nonlinear dynamic equation is solved numerically by the Newmark method and the Newton–Raphson iterative technique. Following a linear analysis, construction of bifurcation diagrams has shown that chaotic motions do indeed occur in the nonlinear system, both with and without harmonic excitation. The route to chaos is shown to be a sequence of period-doubling bifurcations. More extensive calculations demonstrate that the effect of the forcing frequency on the dynamical behaviour of the curved pipe is also significant. It ought to be mentioned, parenthetically, that some interesting and unexpected results may occur by analysing the effects of several other key parameters, such as the nonlinear spring stiffness k, the spring location ζ_c, and so on. A detailed study on this topic will be published elsewhere.

Thus, a nonconservative system was found which displays chaotic motions. The analytical pipe model developed here is remarkably simple, and the numerical simulations are easy to implement. This system offers the potential for further
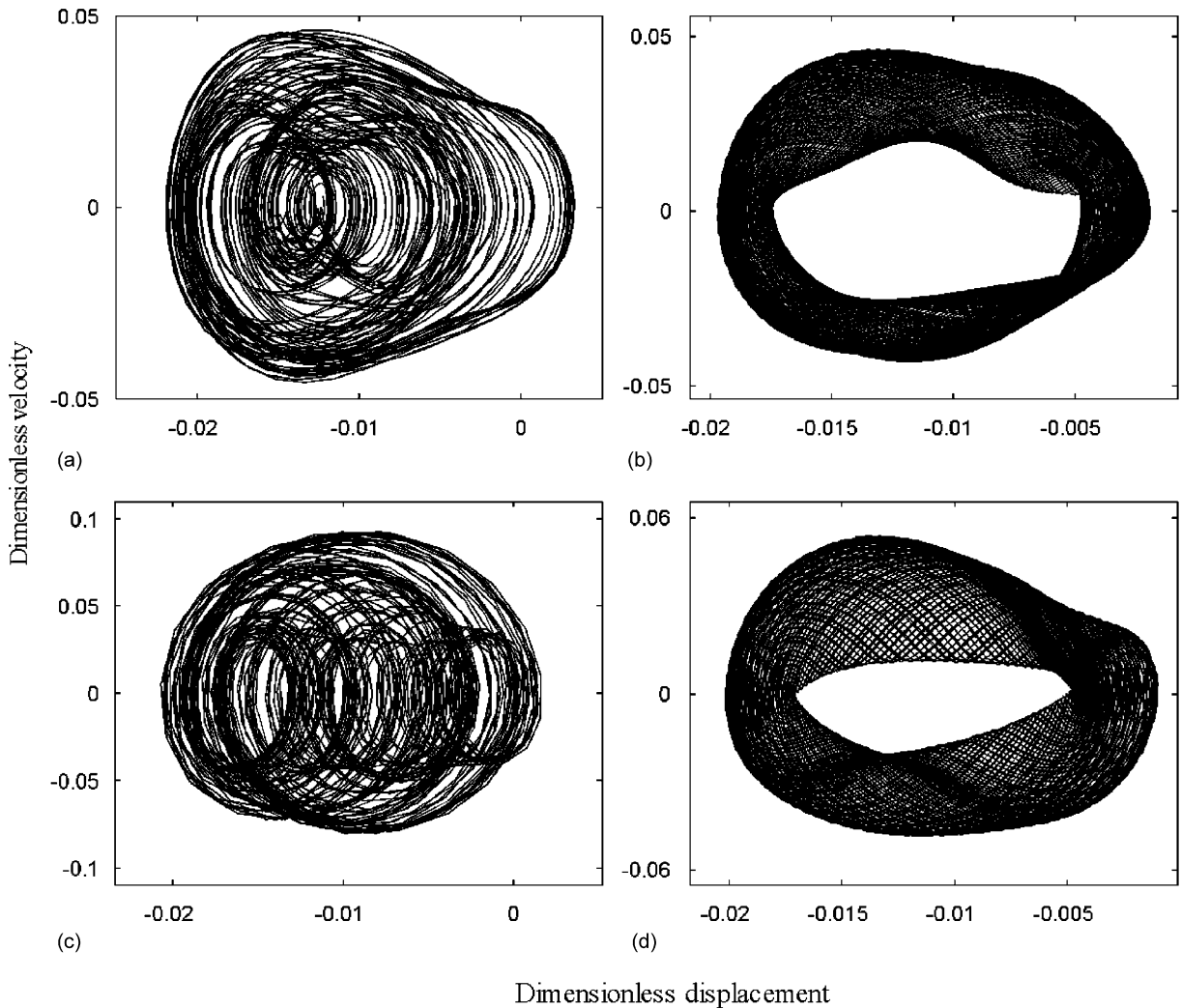
Fig. 13. Phase-plane plots of the free-end deflection of the pipe, for the system defined by $\beta = 0.5$, $k = 1000$, $\xi_c = 0.854$, $N = 12$, $d = 0.005$, $v = 0.27$, and various values of ω. (a) $\omega = 30$, chaotic motion; (b) $\omega = 10.0$, quasi-periodic motion; (c) $\omega = 11.0$, chaotic motion; (d) $\omega = 12.0$, quasi-periodic motion.

and more profound theoretical—experimental study into yet unexplored aspects of its dynamical behaviour—which are currently being investigated.

Acknowledgements

References

Aithal, R., Gipson, G.S., 1990. Instability of internally damped curved pipes. ASCE Journal of Engineering Mechanics 116, 77–90.
Bert, C.W., Malik, M., 1996. Differential quadrature method in computational mechanics: A review. Applied Mechanics Reviews 49, 1–27.

Chen, S.S., 1972a. Flow-induced in-plane instabilities of curved pipe. Nuclear Engineering and Design 23, 29–38.

Chen, S.S., 1972b. Vibration and stability of a uniformly curved tube conveying fluid. Journal of Acoustical Society of America 51, 223–232.

Chen, S.S., 1973. Out-of-plane vibration and stability of curved tubes conveying fluid. Journal of Applied Mechanics 40, 362–368.

Dupuis, C., Rousselet, J., 1985. Application of the transfer matrix method to non-conservative systems involving fluid in curved pipes. Journal of Sound and Vibration 98, 415–429.

Dupuis, C., Rousselet, J., 1992. The equations of motion of curved pipes conveying fluid. Journal of Sound and Vibration 153, 473–489.

Ko, C.L., Bert, C.W., 1984. Non-linear vibration of uniformly curved, fluid-conveying pipes. In: Proceedings of the Fifth International Conference on Pressure Vessel Technology, San Francisco, CA, pp. 469–477.

Ko, C.L., Bert, C.W., 1986. A perturbation solution for non-linear vibration of uniformly curved pipes conveying fluid. International Journal of Non-linear Mechanics 21, 315–325.

Love, A.E.H., 1927. A Treatise on the Mathematical Theory of Elasticity, fourth ed. Dover, New York.

Misra, A.K., Païdoussis, M.P., Van, K.S., 1988a. On the dynamics of curved pipes transporting fluid, part I: inextensible theory. Journal of Fluids and Structures 2, 221–244.

Misra, A.K., Païdoussis, M.P., Van, K.S., 1988b. On the dynamics of curved pipes transporting fluid, part II: extensible theory. Journal of Fluids and Structures 2, 245–261.

Ni, Q., Huang, Y., 2000. Differential quadrature method to stability analysis of pipes conveying fluid with spring support. Acta Mechanica Solida Sinica 13, 320–327.

Païdoussis, M.P., 1998. Fluid–Structure Interactions: Slender Structures and Axial Flow, vol. 1. Academic Press, London.

Timoshenko, S.P., Gere, J.M., 1961. Theory of Elastic Stability, second ed. McGraw-Hill, New York.